



Universiteit
Leiden
The Netherlands

Superstructures of lipids and graphene

Macedo Coelho Lima, L.

Citation

Macedo Coelho Lima, L. (2019, May 23). *Superstructures of lipids and graphene*. Retrieved from <https://hdl.handle.net/1887/73614>

Version: Not Applicable (or Unknown)

License: [Leiden University Non-exclusive license](#)

Downloaded from: <https://hdl.handle.net/1887/73614>

Note: To cite this publication please use the final published version (if applicable).

Cover Page



Universiteit Leiden



The handle <http://hdl.handle.net/1887/73614> holds various files of this Leiden University dissertation.

Author: Macedo Coelho Lima, L.

Title: Superstructures of lipids and graphene

Issue Date: 2019-05-23

CHAPTER 5

Assembly and structural characterization of lipids on graphite and on graphene

Lipids organize in distinct molecular assemblies on graphene, depending on their chemical structure, the substrate underneath graphene and the experimental conditions used for lipid deposition. Using infrared (IR) spectroscopy and quartz crystal microbalance with dissipation monitoring (QCM-D), the formation and structure of lipids with different charges, saturations and chains lengths deposited on graphene was studied systematically. The IR study revealed that saturated lipids exhibited a higher molecular order structure on the graphene surfaces compare to unsaturated lipids, where cationic unsaturated lipids yielded a more organized lipid assembly in comparison to the zwitterionic and anionic unsaturated lipids. QCM-D measurements revealed the wetting transparency effect on the assembly of zwitterionic lipids on graphene with different supporting materials: the formation of a lipid bilayer on graphene transferred on SiO₂ and the adsorption of intact liposomes on graphene transferred on gold. Understanding how a set of different lipids interact and assemble on the surface of graphene transferred on different substrates revealed that the wetting transparency phenomena also impact how lipids interact with graphene.

Publication in preparation: Lia M. C. Lima, Xiaoyan Zhang and Grégory F. Schneider.

5.1 Introduction

Several discrepancies exist regarding how lipids of different molecular composition assemble on the basal plane of graphene.¹⁻⁸ Some papers claim the formation of lipid bilayers,^{1-2, 4, 6} whereas others report the formation of a lipid monolayer^{3, 5, 7-8} with hydrophobic chains facing graphene. Moreover, very few lipids were studied, limiting the scope of understanding of what chemical building blocks in lipids drive their assembly on graphene. So far, lipids were typically assembled on graphene using the vesicle fusion (VF) method¹⁻⁶ or using the so-called dip-pen nanolithography technique,⁷⁻⁸ where lipids such as 1-palmitoyl-2-oleoyl-*sn*-glycero-3-phosphocholine (POPC) or 1,2-diphytanoyl-*sn*-glycero-3-phosphocholine (DPhPC) tend to form a lipid bilayer, while 1,2-dioleoyl-*sn*-glycero-3-phosphocholine (DOPC) and 1,2-dioleoyl-3-trimethylammonium-propane (DOTAP) lead to the formation of a lipid monolayer. Notably, the wetting transparency of graphene⁹ was suggested to play a role on the formation of a lipid bilayer on graphene particularly in the case where graphene has been transferred on hydrophilic substrates.² In addition, the typical characterization methods used to characterize the lipid-graphene structures only comprise fluorescence microscopy and atomic force microscopy (AFM) techniques.

Here, four different lipids were incubated on graphite and graphene using the VF and the Langmuir-Schaefer (LS) methods and were characterized by infrared (IR) spectroscopy and quartz crystal microbalance with dissipation monitoring (QCM-D).¹⁰ In the VF method,¹¹ liposomes are formed, deposited and adsorbed on solid substrates until the lipid vesicles rupture and form a stable layer on the surface of the substrates.¹² The formation and rupture of the lipids on a surface depends on several parameters such as temperature,¹³ vesicle size,¹⁴ buffer solution,¹⁵ vesicle-vesicle interactions¹⁶ and the interactions between the vesicles and the substrate.¹¹ In the LS technique however, the lipids are compressed on a Langmuir trough until a desired surface pressure is reached, and then transferred onto a solid substrate by contacting the substrate horizontally with the lipid monolayer floating at the surface of the Langmuir trough (see Appendix IV for experimental details). IR spectroscopy was used to analyze the structure, order and stability of the lipids assembled using LS and VF methods on chemical vapor deposition (CVD) graphene-on-copper, and on highly oriented pyrolytic graphite (HOPG) substrates.

QCM-D is a unique technique that allows to study dynamic processes at the interface between a solid and a liquid. Over the past two decades, QCM was largely used to study, for instance the formation of lipid monolayers and bilayers on metals, SiO₂ or gold substrates.¹⁰ QCM-D has however not yet been systematically used to study lipid-graphene interactions.^{3,17} As described in Chapter 2 and 3, lipids can form stable structures using the Langmuir-Blodgett technique if graphene is assembled on top, particularly graphene on monolayers of lipids and graphene encapsulated in the hydrophobic core of a lipid bilayer. Dynamic studies (i.e., the kinetics of lipids interacting with graphene, for example with the VF method) are best accessible using QCM-D. In addition, the effect of the wetting transparency on how lipids – from liposomes – rupture on graphene transferred onto different substrates was investigated systematically. CVD graphene was transferred on SiO₂ and on gold QCM crystal sensors using the standard PMMA assisted transfer method.¹⁸ Distinct lipids presented different assemblies on graphene and the wetting transparency also played a role on how lipids arranged on the surface of graphene.

5.2 Results and discussion

In a Langmuir trough, 1,2-dipalmitoyl-*sn*-glycero-3-phosphocholine (DPPC), 1,2-dioleoyl-*sn*-glycero-3-phosphocholine (DOPC), 1,2-dioleoyl-3-trimethylammonium-propane (DOTAP) and 1,2-dioleoyl-*sn*-glycero-3-phospho-L-serine (DOPS) lipids were dropwise deposited at the air-water interface from a chloroform-methanol solution, and compressed to a surface pressure (π) of 30 mN/m and transferred using the LS method to different substrates (Figure 5.1a), namely HOPG and graphene-on-copper. DPPC is in a gel phase at room temperature and presents characteristic phase states upon compression: a gaseous state for π close to 0 mN/m, a solid state for $\pi \sim 30$ mN/m, passing through a plateau – $\pi \sim 10$ mN/m – where the lipid molecules undergo a transition from a fluidic to a condensed phase (Figure 5.1a, solid line).¹⁹ DPPC has a phase transition temperature of 41 °C, DOPC of -20 °C, DOTAP of 0 °C and DOPS of -11 °C all with chains composed of 18 carbons, except for DPPC (16 chains composed of carbon).²⁰⁻²² In the VF method, the liposomes are deposited and ruptured (or adsorbed) on the surface of different substrates forming e.g., supported lipid bilayers (Figure 5.1b, top) or supported lipid monolayers (Figure 5.1b, bottom), depending on the properties of the substrates (for instance, gold vs SiO₂).¹⁷

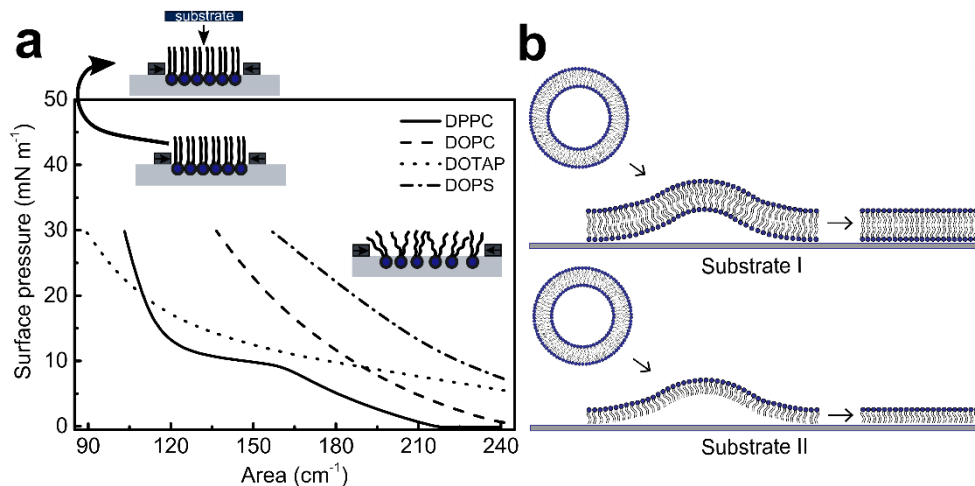


Figure 5.1. Different experimental protocols, namely Langmuir-Schaefer (LS) and vesicle fusion (VF) yielding the formation of a lipid monolayer and bilayer on solid substrates. a) Surface pressure-area isotherms of DPPC, DOPC, DOTAP and DOPS lipids and the subsequent transfer of the compressed lipids to a substrate by the LS method. b) Schematic representation of the possible formation of supported lipid bilayers (top) or supported lipid monolayers (bottom) by VF on substrates.

To study the lipid assembly, different parameters were investigated. The chemical structure of the lipids (Figure 5.2a), the influence of the hydrophobicity of four different substrates (graphene-on-copper, HOPG, graphene-on-SiO₂ and graphene-on-gold), and the difference on the experimental protocol to deposit the lipids (LS or VF).

To assess the structural information and organization of the four types of lipids on graphene-on-copper and HOPG, attenuated total reflectance infrared spectroscopy (ATR-IR) was performed. ATR-IR data was collected for the four different lipids transferred on graphene-on-copper, and on HOPG by the LS and VF methods (black and red respectively, Figure 5.2b). The absorbance peaks of the symmetric and asymmetric CH₂ stretching vibration band were fitted with a Gaussian model and the wavenumbers of the maximum were plotted against the experimental conditions (for at least seven different samples for each condition, see Appendix IV and Figure IV.1 for details). All the samples were measured in a dry state. The absorption bands of the lipid acyl chains are known to vary if the

physical properties of the lipids change.²³ An upward wavenumber shift of the absorption bands corresponds to an increase in disorder of the hydrocarbon chains, and consequently an increase of the lipid mobility within the monolayer/bilayer.²⁴ As expected, the saturated DPPC presented a more ordered structure in comparison with the other three unsaturated lipids independently of their charge (zwitterionic, cationic or anionic), due to the well-organized lipid chains all in a *trans* configuration.²⁵ Unsaturated alkene bonds in the lipid chains promoted a higher degree of disorder due to an increase of the *gauche* conformers in the lipid chains²⁶ and therefore an upward shift of the wavenumbers (Figure 5.2b). Notably, the cationic unsaturated DOTAP lipid presented a higher molecular stability in comparison with the zwitterionic unsaturated DOPC and the anionic DOPS. The unsaturated lipids studied here possess the same chains length and two unsaturated alkene bonds, thus the difference can only be attributed to the composition of the head groups and particularly their charges. A previous study⁵ highlighted that the cationic DOTAP lipid forms a continuous and stable lipid layer on graphene on Si/SiO₂ using the VF method, whereas negatively charged lipids did not interact (i.e. no assembly) on graphene. In fact, in this work the anionic DOPS showed in general a lower structural order compared to the other lipids studied, independently of the substrate or the experimental assembly protocol, as revealed by the shift of the CH₂ stretching bands to higher wavenumbers (Figure 5.2b).

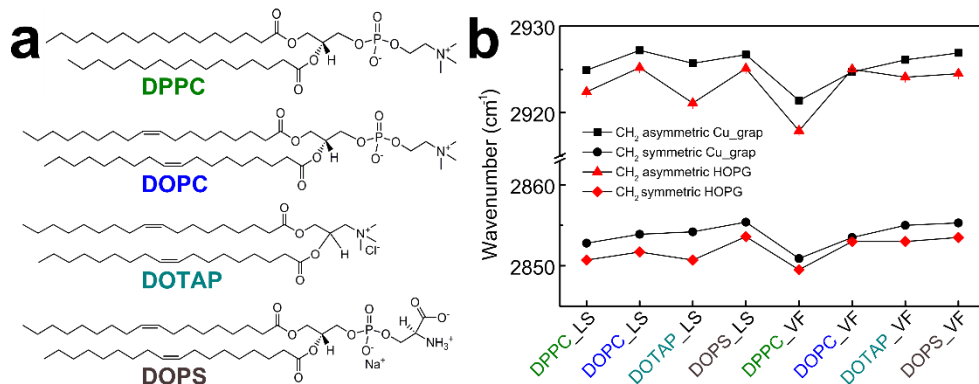


Figure 5.2. Lipid structures and wavenumbers of the CH₂ vibrations infrared absorbance peaks for the four lipid studied and deposited on graphene-on-copper and on highly oriented pyrolytic graphite (HOPG) using vesicle fusion (VF) and Langmuir-Schaefer (LS). a) Molecular structure of DPPC, DOPC, DOTAP and DOPS. b) Mean distribution of the ATR-IR wavenumbers of the symmetric and asymmetric CH₂ vibration peaks for DPPC, DOPC, DOTAP and DOPS lipids transferred by the Langmuir-Schaefer (LS) and the vesicle fusion (VF) methods on graphene-on-copper and HOPG.

The lipids deposited on HOPG presented a higher molecular packing compared to the lipids on graphene-on-copper, independently of the experimental method used (i.e. LS or VF, Figure 5.2b). This is attributed to the disparity in roughness between the supporting substrates.²⁷⁻²⁸ In fact, graphene grown on a copper foil has a considerable high roughness²⁹ in comparison with HOPG, which is atomically flat although constituted of small different layered terraces.³⁰ The AFM topography image of graphene-on-copper presented a roughness of 28.3 nm with folds and pleats (Figure 5.3a), whereas HOPG showed a roughness of 2.3 nm with very flat and continuous flakes (Figure 5.3b). The solid support, particularly the roughness,^{11, 31-32} the surface charge of the substrate and consequently also the ions and pH of the buffer solution,³³⁻³⁴ among others,³⁵⁻³⁶ influence the morphology of the resulting lipid layer. Additionally, the wetting properties, i.e. hydrophobic/hydrophilic^{12, 37} have also a very important role on the formation of a lipid layer.

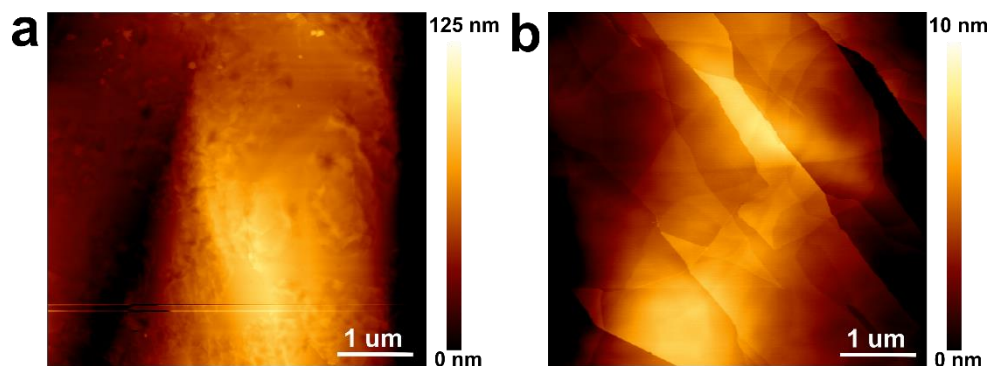


Figure 5.3. AFM intermittent contact mode images in air at room temperature. a) Graphene on a copper foil. b) Highly oriented pyrolytic graphite (HOPG) freshly exfoliated.

In order to investigate and understand the dynamics of vesicle fusion at the interface of a graphene layer, QCM-D experiments were performed. SiO₂-coated and gold-coated QCM crystals were used as substrates for the measurements. CVD graphene was transferred on top of both QCM crystals to investigate the interactions between the different liposomes and graphene. The influence of the substrates underneath graphene were also studied.

Liposomes in a phosphate buffer solution (PBS) were injected 20 minutes (Figure 5.4i) after preparation and were in contact with the substrate using a continuous flow (60 μL/minute) of liposomes for ~1 hour. After, the assembly on graphene was rinsed with PBS (Figure 5.4ii). The change in the resonance frequency of the quartz crystal (Δf) was used to quantify the amount of lipids adsorbed on the graphene.

The zwitterionic saturated DPPC liposomes showed a drop of the resonance frequency, indicating the adsorption of the liposomes on the surface which ruptured to form a lipid bilayer (based on Sauerbrey fitting the layer thickness was 3-4 nm, see appendix for details) on top of graphene-on-SiO₂ (Figure 5.4a). The lipid bilayer was stable for ~6 minutes but at ~26 minutes a sudden drop to a lower frequency (-70 Hz) was observed, indicating that other liposomes or even small air bubbles adsorbed on the surface, also creating a high increase on the energy dissipation values (in red). In contrast, liposomes composed of the cationic unsaturated DOTAP, showed an instant frequency drop to ~-220 Hz with the exact

opposite direction of the energy dissipation values. This indicates that the liposomes did not rupture on top of graphene-on-SiO₂, but rather remained as intact vesicles adsorbed on the graphene surface (Figure 5.4b). The anionic DOPS liposomes showed an increase in frequency and a decrease of the energy dissipation values, indicating that the liposomes did not interact with the surface of graphene (Figure 5.4c). The non-adsorption of DOPS liposomes was also observed in previous studies, where negatively charged liposomes could not deposit on the surface of graphene.⁵

Surprisingly, the QCM-D data showed different results compared to the ATR-IR experiments primarily due to the differences of the solid supports (graphene-on-copper and HOPG are not available as substrates for the QCM measurements), and additionally, the samples for ATR-IR experiments were measured in air (and not in liquid as for QCM-D), likely changing the conformation structure of the lipids.

Finally, the wetting transparency of graphene was investigated using DOPC liposomes deposited on graphene transferred on SiO₂ and on gold substrates. As control experiments, DOPC liposomes were first tested on plain SiO₂ and on plain gold, without the transfer of graphene on top. Liposome rupture resulted in the formation a lipid bilayer on the surface of SiO₂, with a layer thickness of around 4 nm based on Sauerbrey fit. In contrast, DOPC liposomes adsorbed and remained intact on the surface of gold without rupturing (Appendix IV, Figure IV.2). These results are in agreement with literature.¹⁷ For a graphene transferred on a SiO₂ substrate, the liposomes ruptured and formed a lipid bilayer with a layer thickness of 3-4 nm based on Sauerbrey fit (Figure 5.4d), on a graphene-on-gold substrate, the liposomes adsorbed on the surface of graphene without rupturing (Figure 5.4e). The results are similar for graphene-on-SiO₂ and graphene-on-gold compared to SiO₂ and gold alone, suggesting the wetting transparency of graphene, where graphene is transparent to the wetting properties of the substrate underneath.

All graphene sheets transferred on the sensors were characterized by Raman spectroscopy, before and after the QCM-D measurements in order to confirm the transfer of a single layer graphene and the integrity of graphene after the measurements (see plots on Appendix IV, Figure IV.3).

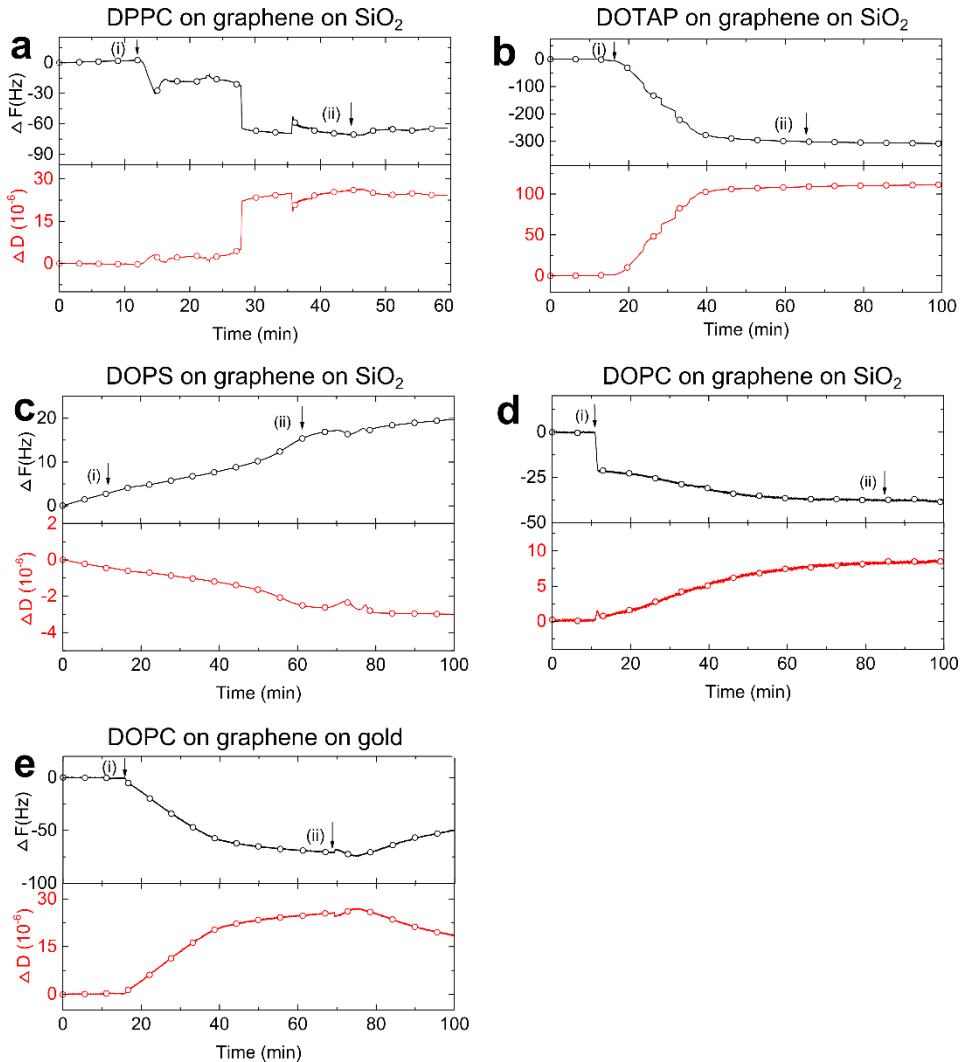


Figure 5.4. Dynamics of liposomes interactions with graphene monitored by quartz crystal microbalance with dissipation monitoring (QCM-D). a) Assembly of the zwitterionic saturated DPPC lipids on graphene-on- SiO_2 . b) Assembly of the cationic unsaturated DOTAP lipids on graphene-on- SiO_2 . c) Assembly of the anionic unsaturated DOPS lipids on graphene-on- SiO_2 . d) Assembly of the zwitterionic unsaturated DOPC lipids on graphene-on- SiO_2 . e) Assembly of the zwitterionic unsaturated DOPC lipids on graphene-on-gold.

5.3 Conclusions

This study elucidates how distinct lipids (DPPC, DOPC, DOTAP and DOPS) assemble on graphite (in the form of HOPG), graphene-on-copper, graphene-on-SiO₂ and graphene-on-gold. ATR-IR results showed that saturated DPPC lipids presented a more ordered structure on the surface of graphene compared to unsaturated lipids, due to a higher rigidity of the lipid acyl chains. For the unsaturated lipids, the cationic DOTAP yielded a higher packed assembly in comparison with the other two unsaturated lipids, i.e. DOPC and DOPS. The anionic DOPS showed a higher fluidity compared to the other lipids. Nevertheless, all the samples were dried in air before the measurements, possibly changing the molecular conformation of the lipids.

Using QCM-D the interactions of the same lipids from liposome solutions were studied for graphene-on-SiO₂ and graphene-on-gold substrates. DPPC liposomes ruptured on the surface of graphene-on-SiO₂ primarily forming a lipid bilayer (similarly to control experiments with plain SiO₂). The cationic DOTAP liposomes adsorbed and remained intact on the surface of graphene whereas the anionic DOPS liposomes did not interact nor adsorbed on graphene-on-SiO₂. The wetting transparency of graphene therefore played a role on the conformational structure of DOPC liposomes, forming a lipid bilayer on graphene transferred on SiO₂ (i.e. hydrophilic), and adsorbed without rupturing on graphene transferred on hydrophobic gold substrate.

In conclusion, distinct lipids interact differently with graphene materials depending on their charge, saturation, structure, on the experimental method used, and on the wetting properties of the solid supports. This work now unifies all the studies reported so far for lipids interacting with graphene transferred on different substrates.

5.4 References

1. Ang, P. K.; Jaiswal, M.; Lim, C. H. Y. X.; Wang, Y.; Sankaran, J.; Li, A.; Lim, C. T.; Wohland, T.; Barbaros, Ö.; Loh, K. P., A bioelectronic platform using a graphene–lipid bilayer interface. *ACS Nano* **2010**, *4* (12), 7387-7394.
2. Wang, Y. Y.; Pham, T. D.; Zand, K.; Li, J.; Burke, P. J., Charging the quantum capacitance of graphene with a single biological ion channel. *ACS Nano* **2014**, *8* (5), 4228–4238.
3. Tabaei, S. R.; Ng, W. B.; Cho, S.-J.; Cho, N.-J., Controlling the formation of phospholipid monolayer, bilayer, and intact vesicle layer on graphene. *ACS Appl. Mater. Interf.* **2016**, *8* (18), 11875-11880.
4. Kuo, C.-J.; Chiang, H.-C.; Tseng, C.-A.; Chang, C.-F.; Ulaganathan, R. K.; Ling, T.-T.; Chang, Y.-J.; Chen, C.-C.; Chen, Y.-R.; Chen, Y.-T., Lipid-modified graphene-transistor biosensor for monitoring amyloid- β aggregation. *ACS Appl. Mater. Interf.* **2018**, *10* (15), 12311-12316.
5. Blaschke, B. M.; Böhm, P.; Drieschner, S.; Nickel, B.; Garrido, J. A., Lipid monolayer formation and lipid exchange monitored by a graphene field-effect transistor. *Langmuir* **2018**, *34* (14), 4224-4233.
6. Connelly, L. S.; Meckes, B.; Larkin, J.; Gillman, A. L.; Wanunu, M.; Lal, R., Graphene nanopore support system for simultaneous high-resolution afm imaging and conductance measurements. *ACS Appl. Mater. Interf.* **2014**, *6* (7), 5290-5296.
7. Hirtz, M.; Oikonomou, A.; Georgiou, T.; Fuchs, H.; Vijayaraghavan, A., Multiplexed biomimetic lipid membranes on graphene by dip-pen nanolithography. *Nat. Commun.* **2013**, *4*, 2591.
8. Hirtz, M.; Oikonomou, A.; Clark, N.; Kim, Y.-J.; Fuchs, H.; Vijayaraghavan, A., Self-limiting multiplexed assembly of lipid membranes on large-area graphene sensor arrays. *Nanoscale* **2016**, *8* (33), 15147-15151.

9. Rafiee, J.; Mi, X.; Gullapalli, H.; Thomas, A. V.; Yavari, F.; Shi, Y.; Ajayan, P. M.; Koratkar, N. A., Wetting transparency of graphene. *Nat. Mater.* **2012**, *11*, 217–222.
10. Cho, N.-J.; Frank, C. W.; Kasemo, B.; Höök, F., Quartz crystal microbalance with dissipation monitoring of supported lipid bilayers on various substrates. *Nat. Protoc.* **2010**, *5*, 1096-1106.
11. Richter, R. P.; Bérat, R.; Brisson, A. R., Formation of solid-supported lipid bilayers: An integrated view. *Langmuir* **2006**, *22* (8), 3497-3505.
12. Jass, J.; Tjärnhage, T.; Puu, G., From liposomes to supported, planar bilayer structures on hydrophilic and hydrophobic surfaces: An atomic force microscopy study. *Biophys. J.* **2000**, *79* (6), 3153-3163.
13. Puu, G.; Gustafson, I., Planar lipid bilayers on solid supports from liposomes – factors of importance for kinetics and stability. *BBA - Biomembranes* **1997**, *1327* (2), 149-161.
14. Jing, Y.; Trefna, H.; Persson, M.; Kasemo, B.; Svedhem, S., Formation of supported lipid bilayers on silica: Relation to lipid phase transition temperature and liposome size. *Soft Matter* **2014**, *10* (1), 187-195.
15. Dacic, M.; Jackman, J. A.; Yorulmaz, S.; Zhdanov, V. P.; Kasemo, B.; Cho, N.-J., Influence of divalent cations on deformation and rupture of adsorbed lipid vesicles. *Langmuir* **2016**, *32* (25), 6486-6495.
16. Zhdanov, V. P.; Dimitrievski, K.; Kasemo, B., Adsorption and spontaneous rupture of vesicles composed of two types of lipids. *Langmuir* **2006**, *22* (8), 3477-3480.
17. Melendrez, D.; Jowitt, T.; Iliut, M.; Verre, A. F.; Goodwin, S.; Vijayaraghavan, A., Adsorption and binding dynamics of graphene-supported phospholipid membranes using the qcm-d technique. *Nanoscale* **2018**, *10* (5), 2555-2567.

18. Li, X.; Zhu, Y.; Cai, W.; Borysiak, M.; Han, B.; Chen, D.; Piner, R. D.; Colombo, L.; Ruoff, R. S., Transfer of large-area graphene films for high-performance transparent conductive electrodes. *Nano Lett.* **2009**, *9* (12), 4359-4363.
19. Lima, L. M. C.; Fu, W.; Jiang, L.; Kros, A.; Schneider, G. F., Graphene-stabilized lipid monolayer heterostructures: A novel biomembrane superstructure. *Nanoscale* **2016**, *8* (44), 18646-18653.
20. Lima, L. M. C.; Giannotti, M. I.; Redondo-Morata, L.; Vale, M. L. C.; Marques, E. F.; Sanz, F., Morphological and nanomechanical behavior of supported lipid bilayers on addition of cationic surfactants. *Langmuir* **2013**, *29* (30), 9352-9361.
21. Picas, L.; Rico, F.; Scheuring, S., Direct measurement of the mechanical properties of lipid phases in supported bilayers. *Biophys. J.* **2012**, *102* (1), L01-L03.
22. Cinelli, S.; Onori, G.; Zuzzi, S.; Bordi, F.; Cametti, C.; Sennato, S.; Diociaiuti, M., Properties of mixed dotap-dppc bilayer membranes as reported by differential scanning calorimetry and dynamic light scattering measurements. *J. Phys. Chem. B* **2007**, *111* (33), 10032-10039.
23. Mitchell, M. L.; Dluhy, R. A., In situ ft-ir investigation of phospholipid monolayer phase transitions at the air water interface. *J. Am. Chem. Soc.* **1988**, *110* (3), 712-718.
24. Lewis, R. N. A. H.; McElhaney, R. N., Membrane lipid phase transitions and phase organization studied by fourier transform infrared spectroscopy. *BBA-Biomembranes* **2013**, *1828* (10), 2347-2358.
25. Garcia-Manyes, S.; Sanz, F., Nanomechanics of lipid bilayers by force spectroscopy with afm: A perspective. *BBA - Biomembranes* **2010**, *1798* (4), 741-749.
26. Tatulian, S. A., Attenuated total reflection fourier transform infrared spectroscopy: A method of choice for studying membrane proteins and lipids. *Biochemistry* **2003**, *42* (41), 11898-11907.

27. Raedler, J.; Strey, H.; Sackmann, E., Phenomenology and kinetics of lipid bilayer spreading on hydrophilic surfaces. *Langmuir* **1995**, *11* (11), 4539-4548.
28. Tero, R., Substrate effects on the formation process, structure and physicochemical properties of supported lipid bilayers. *Materials* **2012**, *5* (12), 2658-2680.
29. Kwon, G. D.; Moyon, E.; Lee, Y. J.; Kim, Y. W.; Baik, S. H.; Pribat, D., Influence of the copper substrate roughness on the electrical quality of graphene. *Mater. Res. Express* **2017**, *4* (1), 015604.
30. Vincent, H.; Bendiab, N.; Rosman, N.; Ebbesen, T.; Delacour, C.; Bouchiat, V., Large and flat graphene flakes produced by epoxy bonding and reverse exfoliation of highly oriented pyrolytic graphite. *Nanotechnology* **2008**, *19* (45), 455601.
31. Cremer, P. S.; Boxer, S. G., Formation and spreading of lipid bilayers on planar glass supports. *J. Phys. Chem. B* **1999**, *103* (13), 2554-2559.
32. Scomparin, C.; Lecuyer, S.; Ferreira, M.; Charitat, T.; Tinland, B., Diffusion in supported lipid bilayers: Influence of substrate and preparation technique on the internal dynamics. *Eur. Phys. J. E* **2009**, *28* (2), 211-220.
33. Richter, R.; Mukhopadhyay, A.; Brisson, A., Pathways of lipid vesicle deposition on solid surfaces: A combined qcm-d and afm study. *Biophys. J.* **2003**, *85* (5), 3035-3047.
34. Redondo-Morata, L.; Oncins, G.; Sanz, F., Force spectroscopy reveals the effect of different ions in the nanomechanical behavior of phospholipid model membranes: The case of potassium cation. *J. Biophys.* **2012**, *102*(1), 66-74.
35. Czolkos, I.; Jesorka, A.; Orwar, O., Molecular phospholipid films on solid supports. *Soft Matter* **2011**, *7* (10), 4562-4576.

36. Reimhult, E.; Höök, F.; Kasemo, B., Intact vesicle adsorption and supported biomembrane formation from vesicles in solution: Influence of surface chemistry, vesicle size, temperature, and osmotic pressure. *Langmuir* **2003**, *19* (5), 1681-1691.
37. González, C. M.; Pizarro-Guerra, G.; Droguett, F.; Sarabia, M., Artificial biomembrane based on dppc — investigation into phase transition and thermal behavior through ellipsometric techniques. *BBA - Biomembranes* **2015**, *1848* (10), 2295-2307.

